Mechanical model of the inspiratory pump

Sergio Basso Ricci, Philippe Cluzel, Andrei Constantinescu, Thomas Similowski

Mechanical model of the inspiratory pump

Sergio Basso Ricci[a], Philippe Cluzel[b], Andrei Constantinescu[a], Thomas Similowski[c,d,*]

[a] *Laboratoire de Mécanique des Solides (CNRS, Polytechnique, Mines, Ponts & Chaussées), Palaiseau, France*
[b] *Service de Radiologie Polyvalente Diagnostique et Interventionnelle, Groupe Hospitalier Pitié-Salpêtrière, Assistance Publique-Hôpitaux de Paris, Paris, France*
[c] *Laboratoire de Physiopathologie Respiratoire, Service de Pneumologie et Réanimation, Groupe Hospitalier Pitié-Salpêtrière, 47-83 Bd de L'Hopital, 75651 Assistance Publique-Hôpitaux de Paris, Paris Cedex 13, France*
[d] *UPRES EA 2397, Université Paris VI Pierre et Marie Curie, Paris, France*

The inspiratory pump (inspiratory muscles and the rib cage) translates inspiratory commands in alveolar ventilation by applying expanding forces to the lungs. Its functioning is of paramount importance to the physiology of breathing and of many pathological situations. Major difficulties in studying its function in relationship with its structure arise from the extremely complex geometrical disposition of its active and passive elements. We herein describe a two-compartment model of the inspiratory pump, with model parameters identification derived from actual measurements obtained by magnetic resonance imaging in normal humans. The equations governing the model are presented. Numerical simulations validate the model by showing a behaviour similar to physiological observations. This opens the possibility of predicting the behaviour of the respiratory system during diseases involving changes in its mechanical or geometrical characteristics.

Keywords: Diaphragm; Respiration; Rib cage; Mathematical model

1. Introduction

The inspiratory pump (inspiratory muscles and rib cage (RC)) translates automatic and voluntary inspiratory commands in alveolar ventilation by applying expanding forces to the lungs. Its correct functioning is of paramount importance to the physiology of breathing and the pathophysiology of many diseases. Studying its function in relationship with its structure is made difficult by the extremely complex geometrical disposition of its active and passive elements. One approach to address this issue relies on imaging techniques to describe the actions of inspiratory muscles through the corresponding geometrical changes (Gauthier et al., 1994; Paiva et al., 1992; Whitelaw, 1987; Whitelaw et al., 1983). Models of various degrees of complexity provide another approach (Angelillo et al., 1997; Ben-Haim and Saidel, 1990; Boriek and Rodarte, 1997; Petroll et al., 1990; Primiano, 1982; Ward et al., 1992). To date, the two strategies do not seem to have been intimately combined.

We hypothesized that the inspiratory pump could be described by a simple model with three degrees of freedom governed by a set of differential equations, and that inputting in this model data obtained from 3D magnetic resonance imaging (MRI) reconstructions and physiological measurements could give access to realistic numerical simulations of its behaviour.

This would open the possibility of predicting the impact of diseases or of therapeutic interventions (e.g. lung volume reduction surgery for emphysema, diaphragm plicature for hemidiaphragmatic paralysis, kyphoscoliosis surgery, or assisted mechanical ventilation, etc.) on the function of the respiratory system.

*Corresponding author. Laboratoire de Physiopathologie Respiratoire, Service de Pneumologie et Réanimation, Groupe Hospitalier Pitié-Salpêtrière, 47-83 Bd de L'Hopital, 75651 Assistance Publique-Hôpitaux de Paris, Paris Cedex 13, France. Tel.: +33-1-42-17-67-61; fax: +33-1-42-17-67-08.

E-mail address: thomas.similowski@psl.ap-hop-paris.fr (T. Similowski).

2. Methods

2.1. Design of the model

2.1.1. Compartments

The proposed model has a RC and an abdominal compartment (AB) (Fig. 1), all the sagittal sections are identical over the right-to-left length d_z. RC includes two rigid elements l_c and l_p, of which the upper one l_c can rotate around its anchor to the rigid vertebral column (angle α) and the lower one l_p can translate horizontally. Abdominal compartment includes two deformable elements l_a and d_a, of which the lower one d_a can translate horizontally, and the anterior one l_a can accomplish a rototranslation, its position being determined by RC and the elongation of the oblique abdominal d_a, (β being the angle between l_a and d_a).

2.1.2. Diaphragm

It is represented by an elastic membrane with an added active muscular component. It has a single insertion line at the back of the inferior RC and its free form is that of a cylindrical dome (Whitelaw et al., 1983). The vertical portion of the dome is apposed to the lower RC, that is thus in relationship with the abdominal cavity. When the diaphragm contracts and descends, the lower RC is exposed through this "zone of apposition" (Zapp) to the resulting positive abdominal pressure, hence its expansion. The height h of Zapp determines the position of the diaphragm. h decreases from residual volume (RV, maximal expiration) to quasi-zero at total lung capacity (TLC, maximal inspiration) (Cluzel et al., 2000). The angle γ defines the incline of the inferior limit of the diaphragm dome over the horizontal, and is used to compute the corresponding volume (Fig. 2).

The geometrical position of the model is determined by three degrees of freedom: the position d_p of RC, that of AB (d_a), and h.

2.2. Forces

2.2.1. Nature

The forces acting on the respiratory system arise from RC muscles (F_p), abdominal muscles (F_{aa}—*transversus abdominis* and F_a—*rectis abdomini*) and the diaphragm (T_{dia}). These forces and the mechanical characteristics of AB and RC determine the abdominal and pleural pressures, p_a and p_p. The muscles are represented in the model by a parallel composition of an active, an

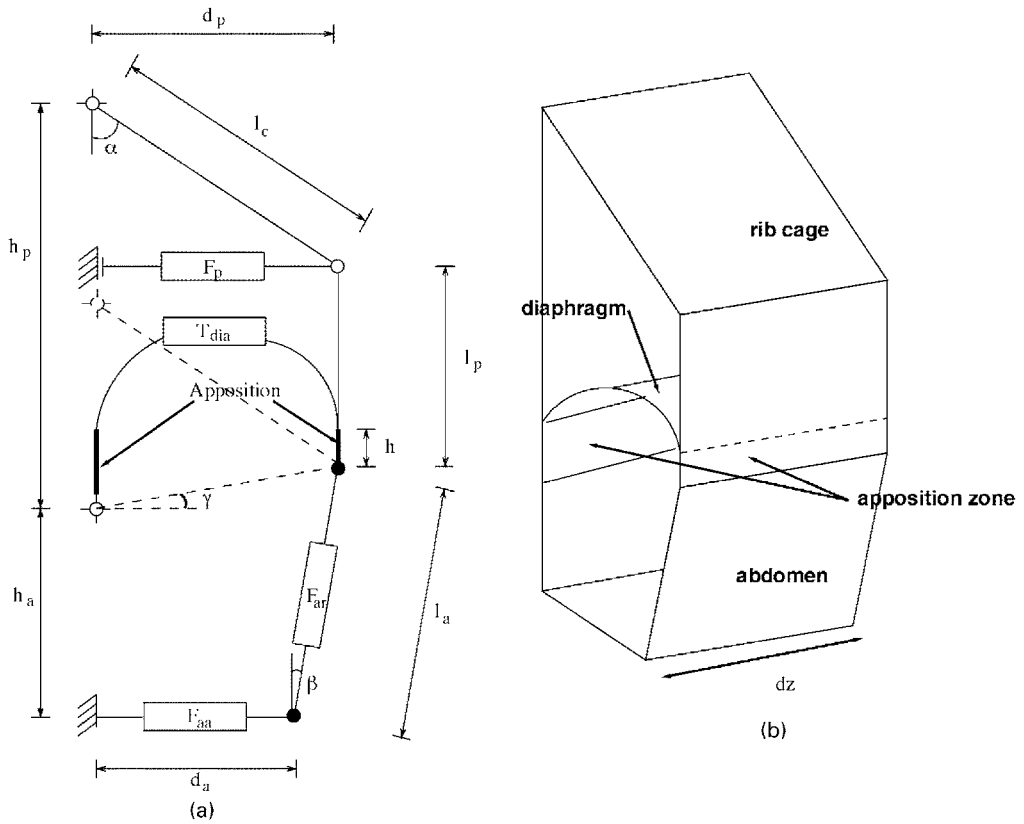

Fig. 1. Panel a is the lateral projection diagram of the model (see Methods, Design of the model, for explanation of the variables and parameters). Panel b shows a 3D sketch of the model, to better put its anatomical correlates in the perspective of the model parameters.

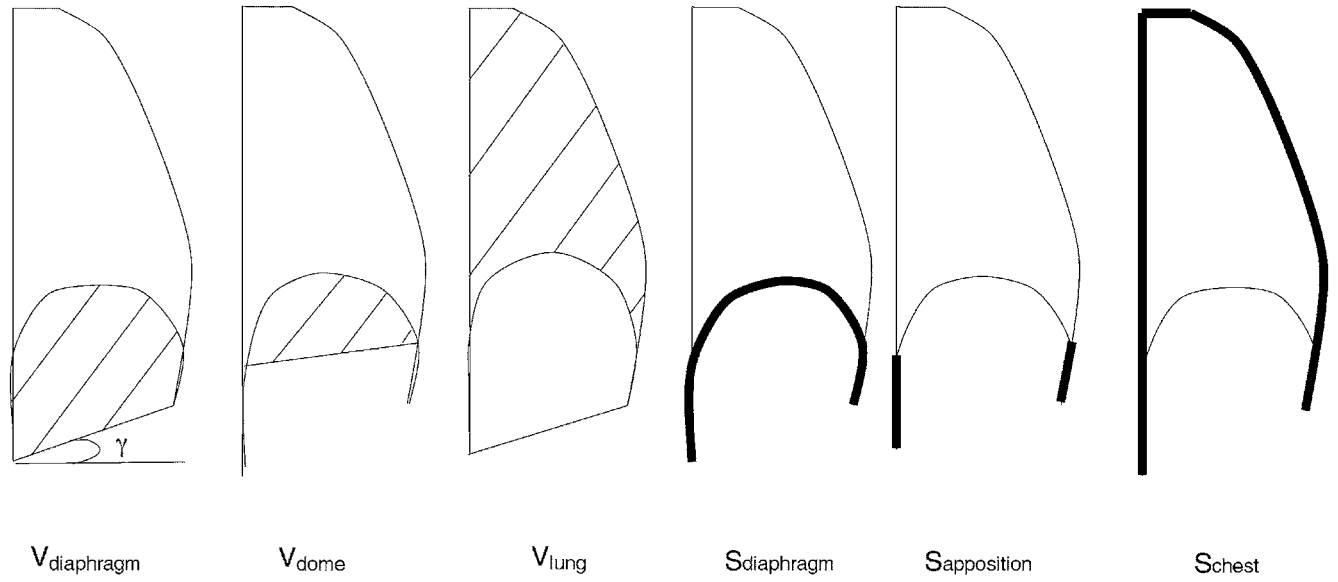

Fig. 2. Schematic representation of the volumes and the surfaces identified by the MRI techniques. From left to right: (1) the rib cage volume under the diaphragm $V_{\text{diaphragm}}$; (2) the volume under the detached part of the diaphragm V_{dome}; (3) the volume of the chest cavity above the diaphragm dome V_{lung}; (4) the total surface of the diaphragm $S_{\text{diaphragm}}$; (5) the surface of the zone of apposition $S_{\text{apposition}}$ and (6) the surface of the thoracic cavity. S_{chest}. $V_{\text{diaphragm}}$ the rib cage volume under the diaphragm (which corresponds approximately to the volume of the portion of the abdominal cavity encompassed by the zone of apposition as defined above), the volume under the detached part of the diaphragm V_{dome} and the volume of the chest cavity above the diaphragm dome V_{lung}; the total surface of the diaphragm $S_{\text{diaphragm}}$, the surface of the zone of apposition $S_{\text{apposition}}$ and the surface of the total rib cage S_{chest}.

elastic and a viscous element (viscous element neglected for the diaphragm for more simplicity). Consequently, F_{p}, F_{aa}, F_{ar}, and T_{dia} are related to the strains exerted on the muscles by the following constitutive equations (see Fung, 1993; and Enderle et al., 1989):

$$
\begin{aligned}
F_{\text{p}} &= F_{\text{p-at}}(t) + k_{\text{p}}\frac{d_{\text{p}} - l_{0\text{p}}}{l_{0\text{p}}} + B_{\text{p}}\frac{\dot{d}_{\text{p}}}{l_{0\text{p}}},\\
F_{\text{ar}} &= F_{\text{ar-at}}(t) + k_{\text{ar}}\frac{l_{\text{ar}} - l_{0\text{ar}}}{l_{0\text{ar}}} + B_{\text{ar}}\frac{\dot{l}_{\text{ar}}}{l_{0\text{ar}}},\\
F_{\text{aa}} &= F_{\text{aa-at}}(t) + k_{\text{aa}}\frac{d_{\text{a}} - l_{0\text{aa}}}{l_{0\text{aa}}} + B_{\text{aa}}\frac{\dot{d}_{\text{a}}}{l_{0\text{aa}}},\\
T_{\text{dia}} &= T_{\text{dia-at}}(t) + 2k_{\text{d}}\theta\frac{r_{\text{dia}} - l_{0\text{d}}}{l_{0\text{d}}},
\end{aligned}
\tag{1}
$$

with k being the elastic rigidity, B the viscosity, l_0 the reference length of the element, and $F_{\text{p-at}}$, $F_{\text{ar-at}}$, $F_{\text{aa-at}}$, and $T_{\text{dia-at}}$ given functions of time. The symbol "$\cdot$" stands for the total time derivative. The equations take into account both the influence of muscle length on the active force developed and that of the velocity of the shortening.

p_{p} varies with the lung volume V_{lungs} according to a non-linear constitutive relationship $p_{\text{p}} = p_{\text{p}}V_{\text{lungs}}$ that can be derived from the experimental data (De Troyer and Estenne, 1984; Milic-Emili et al., 1964). Similarly, p_{a} depends on the abdominal volume V_{a}, but because of insufficient data, it will be assumed that the abdominal content is incompressible. Note that p_{a} and p_{p} represent the homogenised influence of the organs contained in RC and AB.

2.2.2. Balance

It is expressed by the following system of equations:

$$p_{\text{a}} - p_{\text{p}} = \frac{2T_{\text{dia}}}{d_{\text{p}}}, \tag{2a}$$

$$F_{\text{aa}} = F_{\text{ar}}\sin\beta + 0.5p_{\text{a}}\,l_{\text{a}}\cos\beta, \tag{2b}$$

$$
\begin{aligned}
&\big(F_{\text{p}} + T_{\text{dia}}\sin\gamma + F_{\text{ar}}\sin\beta\\
&\quad - 0.5\,p_{\text{p}}\,l_{\text{p}} - 0.5p_{\text{a}}\,l_{\text{a}}\cos\beta)\cos\alpha\\
&\quad = \Big(\frac{p_{\text{p}}\cos\alpha}{2\sin\alpha}\,l_{\text{p}} + l_{\text{c}} + T_{\text{dia}}\cos\gamma\\
&\quad -F_{\text{ar}}\cos\beta + 0.5p_{\text{a}}l_{\text{a}}\sin\beta\Big)\sin\alpha.
\end{aligned}
\tag{2c}
$$

Eq. (2a) corresponds to Laplace's law, and gives the equilibrium between the pressure difference across the diaphragm, its curvature and its tension. Eqs. (2b) and (2c) describe the equilibrium of the outward horizontal forces in the free nodes (black dots in Fig. 1a) located at the bases of RC and AB.

Using algebraic manipulations, one can transform Eqs. (1) and (2) in a system of two differential equations with three unknowns:

$$
\begin{aligned}
\dot{d}_{\text{p}} &= f(t,\, d_{\text{p}},\, d_{\text{a}},\, h),\\
\dot{d}_{\text{a}} &= g(t,\, d_{\text{p}},\, d_{\text{a}},\, h).
\end{aligned}
\tag{3}
$$

A third equation is obtained by assuming that the contents of the abdomen are incompressible:

$$V_{ab}(d_p, d_a, h) = \text{constant} \quad \text{or} \quad V_{ab}(d_p, d_a, h) = 0. \quad (4)$$

Numerical solutions can be obtained by providing values for the parameters, the initial conditions and the history of active components of the forces. For practical reasons, the system has automatically been generated through symbolic computations and then integrated numerically using *Mathematica* (Maeder, 1991; Wolfram, 1991).

2.3. Input data

Geometrical data sets come from MRI sections of the thorax (see Cluzel et al., 2000) at three lung volumes (RV, TLC, and functional residual capacity—FRC-—relaxation volume at the end of expiration). Various dimensions of the model (Fig. 2, Table 1) have been estimated using non-linear least-squares fit (Table 2) from the FRC and RV volumes and areas (but not TLC values, because of highly non-linear behaviours). The rigidities and resting lengths of the muscles were also identified from RV and FRC, at which the data acquisition was performed on a passive system (balance of forces determined exclusively by elastic forces).

The values of the elastic parameters used for the computations are presented in Table 3.

The values of the viscosity parameter derive from the literature (Fung, 1993).

The active components of the forces have been considered given functions of time (Eqs. set (1)), by analogy with the approach of Coirault et al. (1995).

2.4. Numerical simulations

The behaviour of the model has been tested in response to the application of force histories simulating different patterns of breathing (Fig. 3).

3. Results

3.1. Identified parameters

The identified resting lengths of the various muscles (Table 3) are in the anatomical range. Furthermore, the initial length l_{0p} of RC muscles at RV is always greater than at FRC ($d_p = l_c \sin \alpha_{FRC}$, Table 2), consistent with the physiological reality. Note that RC rigidity has the greatest value, which is consistent with what intuition suggests from simple anatomical considerations. This implies that a given applied energy induces a smaller deformation of RC than of any other element.

3.2. Model behaviour

The model simulates the normal behaviour of the respiratory system. During a normal inspiration, d_p and α increase; RC moving forward and upward, d_a increases; AB increasing in diameter, h decreases; in

Table 1
Volumes (l) and surfaces (m^2) computed from magnetic resonance imaging of the thorax (from Cluzel et al., 2000)[a]

Subject	1	2	3	4	5	6 "average subject"
Characteristics						
Age (yr)	27	29	28	32	33	30
Height (cm)	175	172	190	176	186	180
Weight (kg)	66	75	83	82	87	79
Body mass index ($kg\,m^{-2}$)	21.6	25.4	23.0	26.5	25.1	24.3
FRC						
$V_{diaphragm}$	2.34	2.71	3.06	3.16	3.21	2.9
V_{dome}	0.62	0.468	0.7	0.63	0.77	0.64
V_{lung}	5.03	3.34	5.82	3.62	4.75	4.52
$S_{apposition}$	0.0444	0.0631	0.0586	0.0665	0.0659	0.0597
$S_{diaphragm}$	0.0848	0.0999	0.0993	0.1044	0.1097	0.0996
S_{chest}	0.2203	0.2093	0.2351	0.1987	0.2264	0.2179
RV						
$V_{diaphragm}$	2.69	3.28	3.26	3.18	3.72	3.22
V_{dome}	0.45	0.32	0.51	0.62	0.62	0.50
V_{lung}	3.45	3.12	4.35	3.06	3.86	3.57
$S_{apposition}$	0.0614	0.0776	0.0895	0.0650	0.0848	0.0756
$S_{diaphragm}$	0.0965	0.1114	0.1261	0.1045	0.1253	0.1128
S_{chest}	0.1870	0.1887	0.2371	0.1863	0.2251	0.2048

[a] The sixth subject is fictitious, and obtained by averaging the data from the five "real" ones.

Table 2
Geometrical data identified from MRI measurements (Cluzel et al., 2000)[a]

Subject	1	2	3	4	5	6 "average subject"
d_z (cm)	28	23	30	30	33	29
l_c (cm)	4.2	4	4.2	4.3	4.3	4.3
α FRC (°)	64.2	61.9	64.2	58.4	61.3	61.9
α RV (°)	49.8	51.6	49.8	55.6	52.3	52.1
h_{app} FRC (cm)	3	6.3	3.7	5.3	4.2	4.5
h_{app}RV (cm)	7.1	9.7	8.6	6	7.3	7.8
h_p (cm)	40	49	45	36	38	42
l_p (cm)	28	30	30	22	25	27
h_a (cm)	26	32	29	23	25	27

[a] The sixth subject is fictitious, and obtained by averaging the data from the five "real" ones.

Table 3
Numerical values for the various elastic parameters in the model[a]

Subject	1	2	3	4	5	6 "average subject"
k_p (N m^{-1})	1977	2426	2442	8293	3931	2914
k_{aa} (N m^{-1})	274	309	346	288	336	310
k_{ar} (N m^{-1})	42	51	46	37	40	43
k_d (N m^{-1})	120	200	111	1213	177	177
l_{0p} (cm)	4	3.7	4	3.7	3.	4
l_{0aa} (cm)	3.7	3.3	3.7	3.6	3.7	3.6
l_{0ar} (cm)	20	25	23	18	20	21
l_d (cm)	23	35	26	28	26	27

[a] The sixth subject is fictitious, and obtained by averaging the data from the five "real" ones.

line with the downward piston-like movement of the shortening diaphragm, the volume of the chest increases. Larger forces imply greater muscle deformation and larger volume changes. If diaphragm paralysis is simulated (purely extradiaphragmatic command), the abdominal wall expectedly moves inward (decrease in d_a). Quantitatively, the model is sensitive to input parameters: using the data from subject #4 (rigidity above average) (Tables 2 and 3) leads to d_p variations much smaller than average.

3.3. Validation

The model adequately accounts for the relative contribution of the diaphragm and extradiaphragmatic muscles to inspiration (Fig. 3). When a purely diaphragmatic command is applied, the surface of Zapp varies more than when the command is extradiaphragmatic (3% vs 0.5%). When a combined -normal- command is applied, the change in the RC volume above the diaphragm is almost the same as when the command is purely diaphragmatic (6% vs 5.5%).

Fig. 4 shows that RC and AB dimensions vary in phase during normal respiration, and become out of phase during an active expiration below FRC. This corresponds to physiological observations (De Troyer and Loring, 1995; Konno and Mead, 1967). Fig. 4 also shows that the model adequately exhibits hysteresis in the inspiratory–expiratory loop, in line with the viscous properties of the respiratory system that it includes.

4. Discussion

This study shows that the behaviour of the inspiratory pump can be simulated qualitatively and quantitatively using a combination of geometrical imaging and mathematical modelling.

Many models of the respiratory system have been developed. Primiano (1982) was the first to propose a mathematical description of his two-compartment model, but it assumed many restricting hypotheses . Ben-Haim and Saidel (1990) proposed a more anatomically realistic model, based on a spatial disposition of fixed and moving segments, with equations allowing successful simulations of different respiratory manoeuvres. However, they did not consider the various components of force generation. Ward et al. (1992) developed a model that was the first to account for RC distortability, but they did not generate numerical simulations.

Our model has several strengths. It has two compartments, represents the diaphragm with an active and an elastic component, and takes the zone of apposition into account. The muscle modelisation used is realistic, distinguishing an active, an elastic, and a viscous component. The parameters of the model are largely derived from actual data. Splitting the equations into kinematic, constitutive, and force balance equations provides an improved description of the system. This explains that the model behaviour in response to input data is well tuned to physiological facts.

Our model has also various limitations, leaving room for improvement. The 3D anatomical shapes are practically compressed in a 2D model with a constant third dimension. This oversimplifies the deformation of the RC and forbids to handle left-to-right asymmetries. Choosing a more complex representation (attachments of tendons—Enderle et al. (1989), more detailed diaphragmatic characteristics—Ward et al. (1992)) would alleviate these limitations. In most cases, this does not complicate the mathematical approach, but implies a better knowledge of constitutive parameters. The model does not account for RC distortability, but this could be corrected by introducing a spring between l_c and l_p (Fig. 1) and allowing l_c to move away from the vertical during inspiration. The insufficient data available about the viscous properties of muscles limit the realism of our simulations. Nevertheless, our use of muscle fibre data (Fung, 1993) provides relaxation times compatible with the known relaxation dynamics of the

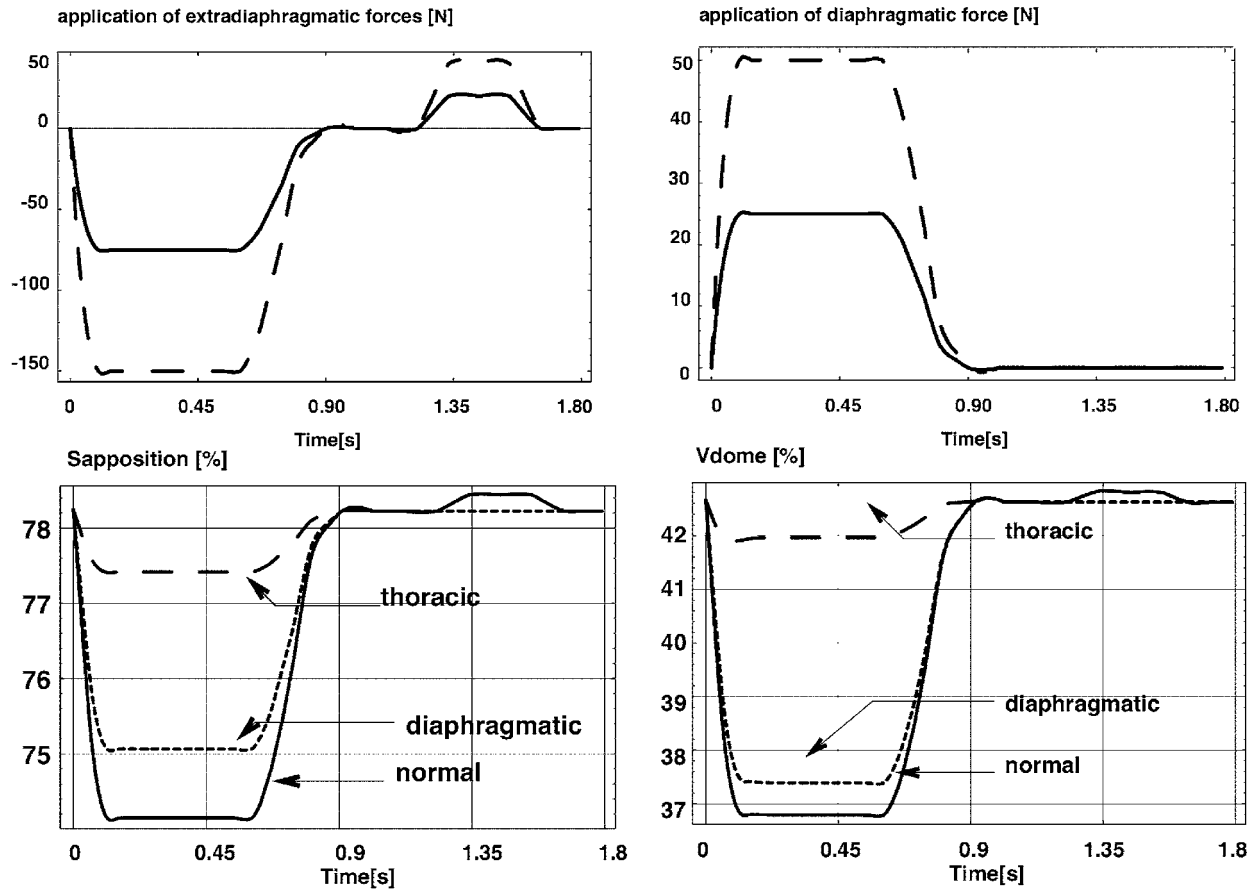

Fig. 3. *Top panels*. Representation of two force histories applied to the model to test its behaviour, one corresponding to an extradiaphragmatic inspiration (left) the other to a pure diaphragmatic inspiration (right). During the inspiratory phase (first half of the time history), no command is given to the abdominal muscles or any other expiratory muscles in order to conform to the physiological behaviour, namely an active inspiration due to inspiratory neuromuscular activity followed by a passive expiration that starts when the inspiratory activity ceases and is solely driven by the elastic recoil of the lung. After the return of the system to functional residual capacity an expiratory command is applied to expiratory rib cage muscles during the second half of the cycle, visible on the left panel as a peak of force whose direction is opposite to that of the preceding inspiratory force. *Bottom panels*. Evolution with time of the surface of the diaphragm apposition zone $S_{\text{apposition}}$ (left) and of the volume under the diaphragm dome V_{dome} (right) in response to a combined diaphragm and extradiaphragmatic inspiratory muscle contraction (“normal”, solid lines), to an isolated diaphragm contraction (“diaphragmatic”, dotted lines) or to an isolated contraction of extradiaphragmatic inspiratory muscles (“thoracic”, dashed lines).

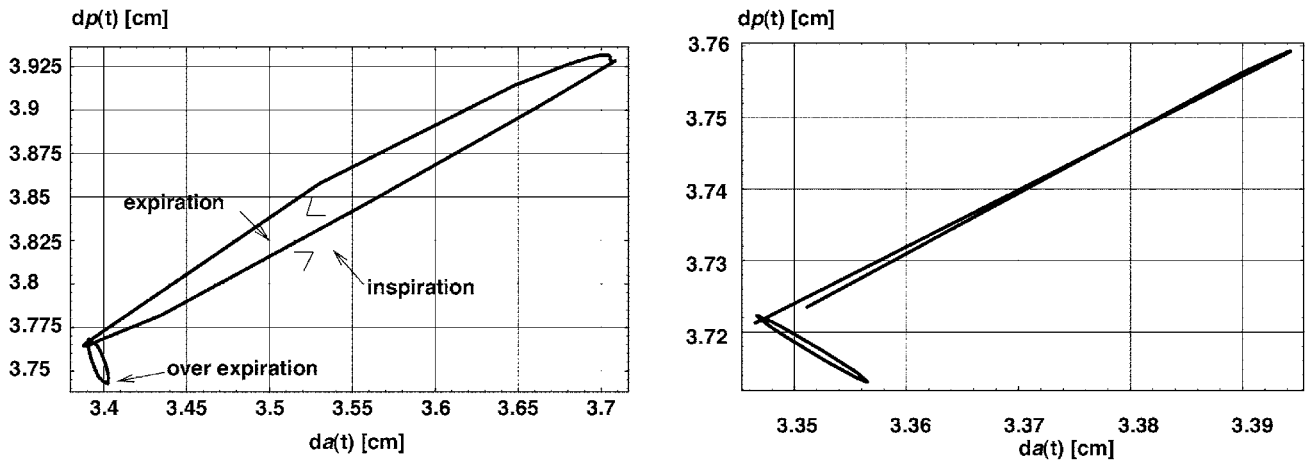

Fig. 4. Chest wall motion ($d_{\text{p}}(t)$, in cm) in relationship with abdominal wall motion ($d_{\text{a}}(t)$, in cm) in the average subject (left panel) and in subject #4, right panel. See the text for details.

respiratory system after a quasi-square wave inspiratory input (phrenic nerve stimulation or ballistic sniff manoeuvre), which is reassuring. Finally, a perfect model would integrate a mathematical description of ventilation, consider the viscoelastic properties of the lungs to account for changes in pressure in the absence of change in volume, and would be stimulated using a precise knowledge of the timing of the commands normally governing inspiratory muscles.

Even before such refinements, the present model should provide a useful tool for computing forces, movements and mechanical properties of the respiratory system and permit a straightforward identification of its parameters from physiological measurements. Coupling it with optimal control or inverse problem techniques could give access, in individual subjects, to internal parameters not directly accessible (e.g. non-specific constitutive relations like lung compliance, airway resistance, or muscle viscosity).

Currently, we submit that the capacity of the model to adequately mimick the behaviour of the respiratory system readily opens the possibility to predict the effects of disease-related changes or, more importantly, of some therapeutic interventions.

Acknowledgements

This work was supported in part by a grant from the French Ministry of Health (PHRC 95-009), a grant from the Societe Francaise de Radiologie, and by the Association pour le Developpement et l'Organisation de la Recherche en Pneumologie (ADOREP), Paris, France.

References

Angelillo, M., Boriek, A.M., Rodarte, J.R., Wilson, T.A., 1997. Theory of diaphragm structure and shape. Journal of Applied Physiology 83, 1486–1491.

Ben-Haim, S.A., Saidel, G.M., 1990. Mathematical model of chest wall mechanics: a phenomenological approach. Annals of Biomedical Engineering 18, 37–56.

Boriek, A.M., Rodarte, J.R., 1997. Effects of transverse fiber stiffness and central tendon on displacement and shape of a simple diaphragm model. Journal of Applied Physiology 82, 1626–1636.

Cluzel, P., Similowski, T., Chartrand-Lefebvre, C., Zelter, M., Derenne, J.-P., Grenier, P., 2000. Magnetic resonance imaging of the diaphragm and chest wall to assess the inspiratory pump. Radiology 215, 574–583.

Coirault, C., Riou, B., Bard, M., Suard, I., Lecarpentier, Y., 1995. Contraction, relaxation, and economy of force generation in isolated human diaphragm muscle. American Journal of Respiration and Critical Care Medicine 152, 1275–1283.

De Troyer, A., Estenne, M., 1984. Coordination between rib cage muscles and diaphragm during quiet breathing in humans. Journal of Applied Physiology 57, 899–904.

De Troyer, A., Loring, S., 1995. Action of the respiratory muscles. In: Roussos, C. (Ed.), The Thorax. Marcel Dekker, New York.

Enderle, J.D., Engelken, E.J., Stiles, R.N., 1989. A linear muscle model predicts the hyperbolic force-velocity relationship. Biomedical Sciences Instrumentation 25, 149–153.

Fung, Y.C., 1993. Mechanical Properties of Living Tissues. Springer, Berlin.

Gauthier, A.P., Verbanck, S., Estenne, M., Segebarth, C., Macklem, P.T., Paiva, M., 1994. Three-dimensional reconstruction of the in vivo human diaphragm shape at different lung volumes. Journal of Applied Physiology 76, 495–506.

Konno, K., Mead, J., 1967. Measurement of the separate volume changes of rib cage and abdomen during breathing. Journal of Applied Physiology 22, 407–422.

Maeder, R., 1991. Programming in Mathematica. Addison-Wesley, Reading, MA.

Milic-Emili, J., Orzalesi, M.M., Cook, C.D., Turner, J.M., 1964. Respiratory thoraco-abdominal mechanics in man. Journal of Applied Physiology 19, 217–233.

Paiva, M., Verbanck, S., Estenne, M., Poncelet, B., Segebarth, C., Macklem, P.T., 1992. Mechanical implications of in vivo human diaphragm shape. Journal of Applied Physiology 72, 1407–1412.

Petroll, W.M., Knight, H., Rochester, D.F., 1990. A model approach to assess diaphragmatic volume displacement. Journal of Applied Physiology 69, 2175–2182.

Primiano Jr., F.P., 1982. Theoretical analysis of chest wall mechanics. Journal of Biomechanics 15, 919–931.

Ward, M.E., Ward, J.W., Macklem, P.T., 1992. Analysis of human chest wall motion using a two-compartment rib cage model. Journal of Applied Physiology 72, 1338–1347.

Whitelaw, W.A., 1987. Shape and size of the human diaphragm in vivo. Journal of Applied Physiology 62, 180–186.

Whitelaw, W.A., Hajdo, L.E., Wallace, J.A., 1983. Relationships among pressure, tension, and shape of the diaphragm. Journal of Applied Physiology 55, 1899–1905.

Wolfram, S., 1991. Mathematica, A System for Doing Mathematics by Computer. Addison-Wesley, Reading, MA.